Available online at www.sciencedirect.com
SCIENCE DIRECT®
Journal of Catalysis 220 (2003) 478–485
JOURNAL OF CATALYSIS
www.elsevier.com/locate/jcat

# The effect of oxide formation on bistability in CO oxidation on Pt

Vladimir P. Zhdanov [a,b,*] and Bengt Kasemo [a]

[a] *Competence Center for Catalysis and Department of Applied Physics, Chalmers University of Technology, S-412 96 Göteborg, Sweden*
[b] *Boreskov Institute of Catalysis, Russian Academy of Sciences, Novosibirsk 630090, Russia*

Received 9 April 2003; revised 16 June 2003; accepted 16 June 2003

**Abstract**

Kinetics of CO oxidation on Pt is bistable both under UHV conditions and at atmospheric pressure. In the former case, the bistability can be explained by using the established reaction scheme, including reversible CO adsorption, dissociative $O_2$ adsorption, and reaction between adsorbed CO and O. Also at higher pressures, this model accounts well for the low-reactive (CO-dominated) regime. However, in the high-reactive (oxygen-rich) regime, the kinetics may be influenced by surface oxide formation at the higher pressures. Our present Monte Carlo simulations illustrate what may happen when oxide formation and removal occur with participation of gas-phase $O_2$ and CO molecules, respectively. Specifically, we show that these relatively slow steps may control the reaction rate in the high-reactive state. In this case, the hysteresis loop is found to be qualitatively similar to that predicted by the conventional reaction scheme, but the $CO_2$ formation rate in this state is appreciably lower. These predictions are in qualitative agreement with the results of recent STM studies of CO oxidation on Pt(110) at atmospheric pressure.


*Keywords:* CO oxidation; Oxide model; Monte Carlo simulations

## 1. Introduction

In CO oxidation on Pt and other Pt-group metals, kinetic bistability has been observed on single crystals, polycrystalline samples, and supported catalysts in a pressure range from $10^{-12}$ bar to atmospheric pressure (see reviews [1–3] and/or typical experiments and mean-field (MF) calculations for Pt(111) [4,5] and Ir(111) [6]). The understanding of this phenomenon is of considerable intrinsic interest and also important for applications. For example, treatment of automotive exhaust gases often occurs under unsteady-state conditions including sequential ignition and extinction periods which are directly related to CO-oxidation bistability. Thus, optimization of the performance of car catalytic converters might need to incorporate an accurate description of the bistability.

To interpret the bistability in CO oxidation on Pt, one has to understand the mechanism of this reaction. In this field, the evolution of the concepts can retrospectively be divided into a few periods. Before and during the formative period of surface science, CO oxidation on the Pt-group metals was generally accepted [7] to occur via the mechanism including reversible CO adsorption,

$$CO_{gas} \rightleftharpoons CO_{ads}, \tag{1}$$

dissociative $O_2$ adsorption,

$$(O_2)_{gas} \rightarrow 2O_{ads}, \tag{2}$$

Langmuir–Hinshelwood (LH) reaction between adsorbed CO and O,

$$CO_{ads} + O_{ads} \rightarrow (CO_2)_{gas}, \tag{3}$$

and Eley–Rideal (ER) reaction between gas-phase CO and adsorbed O,

$$CO_{gas} + O_{ads} \rightarrow (CO_2)_{gas}. \tag{4}$$

The subscripts “gas” and “ads” denote here gas-phase and adsorbed particles, respectively.

Surface-science-based studies have shown that the ER step (4) actually does not occur (at least under UHV conditions). Without step (4), the mechanism above is well known to predict bistability, provided that the LH step (3) is fast. The bistability derives primarily from the difference in the

* Corresponding author.
*E-mail address:* zhdanov@catalysis.nsk.su (V.P. Zhdanov).

0021-9517/$ – see front matter 
doi:10.1016/S0021-9517(03)00276-8

detailed adsorption kinetics of CO and $O_2$. The corresponding MF equations have been successfully used to quantitatively describe the bistability observed on single-crystal surfaces under UHV conditions (see, e.g., Refs. [3–6]). The reaction scheme (1)–(3) has also been employed for MF and Monte Carlo (MC) simulations of the bistable kinetics on nanometer-sized supported particles [8–12]. For much higher but still subatmospheric pressures, the MF equations based on steps (1)–(3) have been used as well in order to describe steady-state and transient reaction kinetics [13–15]. The available experience indicates that with a careful choice of the parameters the model allows reasonably good reproduction of the kinetic phase diagram [15] and accurate simulation of catalytic ignition [14]. The situation with extinction is, however, more complex, because after ignition (at oxygen excess) the system is in the high reactive state and the reaction rate is then often controlled by gas-phase reactant transport, and accordingly the details of the surface chemistry remain open for debate. At our lab, attempts [16] to describe extinction quantitatively (including gas-phase diffusion limitations) indicate that the conventional CO-oxidation scheme appears to significantly overestimate the reaction rate in the high-reactive state.

Complications of the kinetics of CO oxidation at appreciable oxygen excess seem be related to the formation of "surface oxide" or "subsurface oxygen" (these terms are often used interchangeably to denote oxygen species that are not the chemisorbed oxygen identified in UHV experiments) [17]. To our knowledge, this idea was mentioned from time to time in experimental studies of CO oxidation at least since the mid-1970s. Its wide circulation started after publication of the famous paper by Sales, Turner, and Maple [18], in which they complemented their experimental studies of kinetic oscillations in CO oxidation on polycrystalline Pt, Pd, and Ir at atmospheric pressure by a model including surface-oxide formation. At that time, convincing experimental data, supporting the idea that the oscillations were connected with the oxide formation, were lacking. Later on, using LEED, TPD, and XPS, Vishnevskii and Savchenko [19] demonstrated that at low pressures the oxide formation really plays an important role in oscillations on Pt(110), especially during long runs. More recently, Rotermund et al. [20,21] have explicitly observed oxide formation on the micrometer scale during oscillations on Pt(110) under UHV conditions by employing the photoelectron emission microscope (PEEM).

Despite these and other findings (for a review, see Ref. [21]), the understanding of the details of the oxide formation is still limited especially at subatmospheric pressures (one of the reasons is that the interpretation of the results identifying the state of oxygen, e.g., by XPS measurements [22], is often far from straightforward).

The most recent advances are related to Hendriksen and Frenken's atmospheric-pressure STM study [23] of CO oxidation on Pt(110). At CO excess, they observed as expected that the surface is fairly flat [in the $(1 \times 1)$ state]. At $O_2$ excess, at which on the basis of the UHV studies [24] one would expect to observe the $(1 \times 2)$ structure, the surface was, however, found to be rough and presumably covered by a thin coherent oxide film. The kinetic bistability was demonstrated to be apparently similar to that predicted by the conventional reaction scheme (1)–(3), but the interpretation of the high-reactive regime was quite different. Specifically, the catalytic activity was attributed in the latter case exclusively to the interplay of CO reaction with oxygen, forming surface oxide, and adsorption of the gas-phase oxygen at oxide vacancies (this scheme is similar to the conventional mechanism of CO oxidation on oxides [7,25]).

Kinetic models describing the effect of oxide formation on CO oxidation are numerous (see Section 6 in a recent review [26] and Ref. [27]). The main goal of these simulations was, however, to describe kinetic oscillations, which are observed at the boundary between the two reaction regimes. For this reason, the corresponding reaction schemes do not seem to be directly applicable to the situation when the surface is nearly completely covered by an oxide film and the reaction occurs via CO interaction with oxide. More specifically, the available models predict that at $O_2$ excess either the surface is partly covered by chemisorbed oxygen and oxide and the reaction rate is determined primarily by CO interaction with chemisorbed oxygen [step (3)] or the surface is completely covered by oxide and the reaction is not going on. Both these predictions are not in line with the experiment [23].

The main goals of the present work are (i) to construct a relatively simple kinetic model making it possible to mimic a transition from the conventional mechanism of CO oxidation [steps (1)–(3)] at CO excess to the reaction regime including CO interaction with a fully developed surface-oxide overlayer at $O_2$ excess and (ii) to present MC simulations illustrating the special features of bistable kinetics complicated by oxide formation.

## 2. Model

Basically, surface oxide should be treated as a new phase. On Pt, this phase seems to be unstable at low oxygen coverages or kinetic factors prevent its formation at low coverage/low pressure. With increasing coverage, the binding energy of chemisorbed oxygen rapidly decreases due to repulsive lateral O–O interactions and the surface-oxide formation may become favorable (this scenario appears to apply to several metals [28,29]). The details of the kinetics of surface-oxide formation are expected to strongly depend on lateral interactions (for a relevant discussion, see Ref. [30]). The most straightforward way to simulate such kinetics is to construct a generic lattice–gas model, explicitly taking into account lateral interactions. This might be especially useful if oxygen diffusion is very rapid and the chemisorbed and oxide phases are close to equilibrium. During CO oxidation on Pt, the two phases seem, however, to be far from equilib-

rium even under UHV conditions, because oxygen diffusion appears to be slow compared to other steps (see, e.g., the PEEM patterns [20]). Although a lattice model with lateral interactions might be useful in the latter case as well, we believe that in the situation far from equilibrium it makes sense to first employ a simpler approach in order to reduce the number of model parameters and to focus the presentation on the key points. Specifically, it makes sense (i) to take into account the probable type of lateral interactions implicitly by introducing qualitatively sound prescriptions for calculating the probabilities of various processes for different arrangements of adsorbed particles and (ii) to skip inferior details (e.g., the precursor states for CO adsorption). Following this line, we first outline general ingredients of our model and then, describing the MC algorithm, introduce in detail the rules for executing elementary reaction steps.

In our simulations, we analyze the simplest case in which surface-oxide formation occurs in one layer on a $L \times L$ square lattice. Specifically, each lattice site is either vacant or occupied by CO or oxygen. Oxygen may be either in the chemisorbed state or in the oxide state, O and O*, respectively. In reality, e.g., on Pt(110) [23], the surface oxide seems to be thicker. Nevertheless, we believe that the one-layer model may still be applicable, especially under steady-state conditions at subatmospheric pressures, because in this case, due to a slow rate of oxygen diffusion jumps compared to the rates of other processes, the deeper oxide layers are expected to form the environment for the top layer rather than participating in reaction. For this reason, the model including a single oxide layer with different reactivity toward CO than toward chemisorbed oxygen is able to catch the essence of the problem under consideration; if multiple layers are involved it is expected to modify the details of the reaction kinetics, but not the qualitative aspects.

The one-layer oxide model has already been widely used in simulations [18,26]. Usually, the oxide formation and removal are assumed to occur as

$$O_{ads} \rightleftharpoons O^*_{ads}, \tag{5}$$

$$CO_{ads} + O^*_{ads} \rightarrow (CO_2)_{gas}. \tag{6}$$

The STM experiments [23] indicate, however, that under nearly steady-state conditions the oxide layer is rather formed ("formed" is here equivalent to "maintained") via adsorption of the gas-phase oxygen at oxide vacancies,

$$(O_2)_{gas} \rightarrow 2O^*_{ads}. \tag{7}$$

The details of oxide removal are not quite clear from the experiment. Taking into account that the $CO_2$ formation was observed for a well-developed oxide film, one can conclude [23] that the most likely scheme of oxide removal is similar to that occurring on oxides [25], i.e., CO reversibly adsorbs on metal atoms forming the stable surface oxide and then reacts with oxidic oxygen. Basically, this is a LH scheme. The important point is, however, that in this case the sites for CO adsorption cannot be occupied by additional oxygen. In fact, this means that CO adsorption occurs on lattice sites occupied by oxygen forming the oxide. The details of description of this scheme depend on the CO binding energy on the oxide. If the binding energy is appreciable, one should explicitly introduce the corresponding CO coverage. If, however, the binding energy is small as in the case of the Pt oxide, CO adsorbed on the oxide is in equilibrium with the gas phase, the corresponding CO coverage is low, and accordingly the oxide-removal rate is proportional to CO pressure. Mathematically, the latter case is equivalent to the ER reaction with gas-phase CO,

$$CO_{gas} + O^*_{ads} \rightarrow (CO_2)_{gas}. \tag{8}$$

In our simulations, we adopt this *apparent* step. [To some extent, we revive here the old ideas on the role of the ER step in CO oxidation on Pt (see the Introduction). The important difference is, however, that now (i) the ER step is considered to be apparent and (ii) CO reacts with $O^*_{ads}$.]

Our model includes the conventional steps (1)–(3) for CO oxidation. The oxide formation and removal are considered to occur primarily via steps (7) and (8). Focusing on these steps, we neglect step (6). This approximation is in line with the STM observations [23] indicating that during the high-reactive regime at oxygen excess the oxide coverage is appreciable, CO coverage is low, and accordingly channel (8) seems to be more probable. With increasing CO pressure, the oxide coverage decreases, CO adsorption becomes more probable, and accordingly step (6) may become significant (especially during oscillations). Thus, in principle, the model should take into account step (6) as well. This is, however, beyond our present goals.

Steps (5) are admitted but only in the cases in which O has an oxide environment and O* has no such environment, respectively (these rules mimic the tendency of O and O* to form different phases). In addition, we take into account diffusion of adsorbed CO molecules. This process is well known to be rapid compared to other steps [in particular, step (3) is not limited by CO diffusion]. Oxygen diffusion is neglected.

To characterize the relative rates of reaction steps and CO diffusion, we introduce the dimensionless parameters $p_{rea}$. These processes are run with probabilities $p_{rea}$ and $1 - p_{rea}$, respectively. This means that for each MC trial we generate a random number $\kappa$ ($0 < \kappa \leqslant 1$) and try to execute CO diffusion or reaction steps if $\kappa > p_{rea}$ and $\kappa < p_{rea}$, respectively.

For CO diffusion, a site is chosen at random. If the site is vacant or occupied by oxygen, the trial ends. If the site is occupied by CO, one of the nearest-neighbor (nn) sites is selected at random and CO is removed to the latter site provided that it is vacant and has no nn O*. CO jumps to nn vacant sites contacting O* are prohibited because the CO binding energy on such sites is assumed to be low. [The configurations with CO and O* in nn sites may, however, be generated (with a low probability) after execution of step (8) (see below). In such cases, CO is expected to desorb or jump

to vacant nn sites. The details of these events do not influence the reaction kinetics. To avoid nn CO and O* pairs, we complement the rules for CO diffusion by the prescription that a chosen CO molecule is removed from the lattice if it has nn O*. This prescription mimics rapid desorption of CO molecules in the situations in which they are located in sites contacting oxide.]

For reaction steps, a site is chosen at random. Then, depending on its state, there are four routes:

- If the site chosen is vacant, we execute trials of CO adsorption or $O_2$ adsorption [steps (2) and (7)].
  - (i) CO adsorption is performed provided that $\rho < p_{ad}^{CO}$, where $p_{ad}^{CO}$ is the CO adsorption probability and $\rho$ ($0 < \rho \leqslant 1$) is a random number. A trial is accepted if nn sites are free of O*. CO adsorption on vacant sites contacting O* is considered to be negligible because as already noticed above the CO binding energy on such sites is assumed to be low.
  - (ii) A trial of $O_2$ adsorption with formation of chemisorbed oxygen [step (2)] is executed provided that $p_{ad}^{CO} < \rho < p_{ad}^{CO} + p_{ad}^{O_2}$, where $p_{ad}^{O_2}$ is the probability of step (2). In this case, one of the next-nearest-neighbor (nnn) sites is selected at random and the trial is accepted if the latter site is vacant and both sites have no nn O or O*. Using these rules, we consider that O adsorption on nn sites is improbable due to strong lateral O–O repulsion. The presence of oxide in nn sites is assumed to suppress step (2) as well.
  - (iii) For oxide formation [step (7)], one of the nn sites is selected at random. If the latter site is vacant, step (7) is performed provided that

    $$p_{ad}^{CO} + p_{ad}^{O_2} < \rho < p_{ad}^{CO} + p_{ad}^{O_2} + p_1^{ox}$$

    in the case in which the two sites have no nn O* or provided that

    $$p_{ad}^{CO} + p_{ad}^{O_2} < \rho < p_{ad}^{CO} + p_{ad}^{O_2} + p_2^{ox}$$

    in the case in which the two sites have at least one nn O*, where $p_1^{ox}$ and $p_2^{ox}$ are the probabilities of step (7) for the metal and oxide phases, respectively. These prescriptions make it possible to describe a cooperative mode of the oxide growth (i.e., the formation of oxide islands) provided that $p_1^{ox} < p_2^{ox}$.
- If the site chosen is occupied by CO, CO desorption or reaction trial [step (3)] is executed for $\rho < p_{des}$ and $\rho > p_{des}$, respectively. For CO reaction, one of the nn sites is selected at random, and the trial is accepted if the latter site is occupied by O.
- If the site chosen is occupied by O, the oxide formation step, $O_{ads} \to O_{ads}^*$, is executed with the corresponding probability $p_{ox}$ (i.e., if $\rho < p_{ox}$) provided that O has at least two nn O*. This condition is also introduced in order to mimic a cooperative mode of the oxide growth (the choice of the number 2 here is of course somewhat arbitrary).
- If the site chosen is occupied by O*, the apparent ER step (8) is performed if $\rho < p_{ER}$, or the oxide conversion step, $O_{ads}^* \to O_{ads}$, is executed provided that the nn site are free of O* and $p_{ER} < \rho < p_{ER} + p_{red}$ (if $\rho > p_{ER} + p_{red}$, the trial ends). The probability of step (8) is proportional to CO pressure as well as the probability $p_{ad}^{CO}$, characterizing the CO impingement rate. This means that $p_{ER}$ and $p_{ad}^{CO}$ should be related as $p_{ER} = p_r p_{ad}^{CO}$, where $p_r$ is the ratio of the two rates. Practically, the latter means that by changing $p_{ad}^{CO}$ we should simultaneously change $p_{ER}$ proportionally.

To measure time, we use MC steps (MCS). One MCS is defined as $L \times L$ attempts of the adsorption-reaction events on average, i.e., the MC time is calculated by dividing the total number of MC trials by $L \times L$ and multiplying by $p_{rea}$. Simulating these events, we consider that the sum of the probabilities of CO desorption and LH reaction (3) equals unity. This means that the MC and real times are interconnected as $t_{MC} = (k_{des} + k_{LH})t$, where $k_{des}$ and $k_{LH}$ are the corresponding rate constants. In principle, one might define one MCS as $L \times L$ trials of adsorption, reaction, and CO diffusion. In this case, the time scale would primarily be connected with CO diffusion, because in our simulations this process is rapid compared to other steps. If CO diffusion is sufficiently fast, the reaction kinetics becomes in fact independent of the rate of this process. For this reason, in simulations of reaction kinetics it makes no sense to relate MC time to the rate of CO diffusion.

## 3. Results of simulations

The simulations were performed on a $200 \times 200$ lattice with periodic boundary conditions. The values of the kinetic parameters were chosen in qualitative agreement with the experimental data available for CO oxidation on Pt. In particular, the parameters for steps (1) and (2) were fixed as $p_{des} = 0.001$ and $p_{ad}^{O_2} = 0.01$ in order to reproduce a well-developed hysteresis (with increasing $p_{des}$, the hysteresis loop will be narrower and eventually disappear). $p_{ad}^{CO}$ was a governing parameter. CO diffusion was set 10 times faster than the catalytic cycle (further increase of the rate of this process does not change the results).

To explore the bistability, we started from a clean lattice and simulated the steady-state reaction kinetics with stepwise increase or decrease in the governing parameter (CO pressure) by increasing or decreasing $p_{ad}^{CO}$ by $\Delta p_{ad}^{CO}$ after each $10^4$ MCS. This procedure makes it possible to construct a hysteresis loop. The shape of the loop (or, more specifically, the parameter values corresponding to the transitions from one branch to another) slightly depends on $\Delta p_{ad}^{CO}$ and also on the duration of the intervals, $\Delta t$, where $p_{ad}^{CO}$ is kept

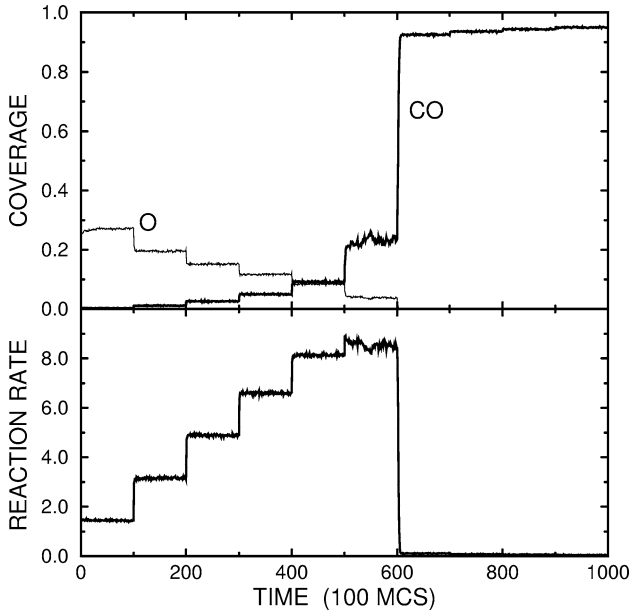


(a)

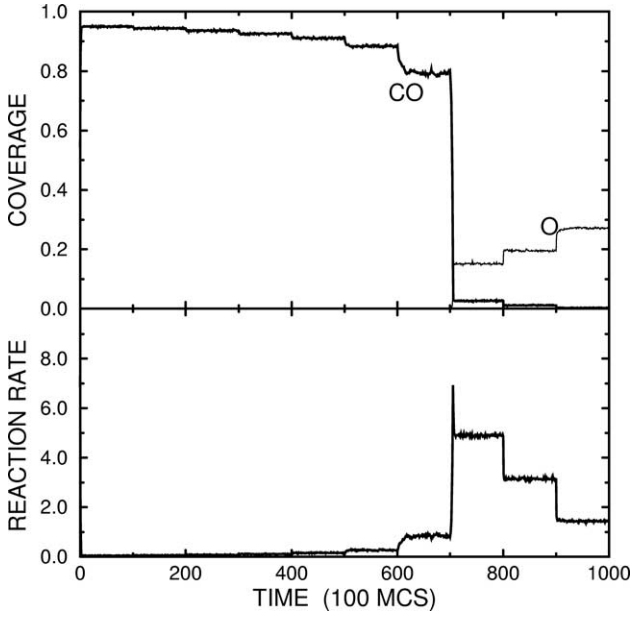


(b)

Fig. 1. Adsorbate coverages (ML) and reaction rate ($10^{-3}$ ML/MCS) for the conventional reaction scheme (no oxide formation) with (a) increasing and (b) decreasing $p_{ad}^{CO}$ (between 0.002 and 0.2) by $\Delta p_{ad}^{CO} = 0.002$ after each $10^4$ MCS. The time interval used to obtain the reaction rate is 100 MCS. The interval between the data points is also 100 MCS.

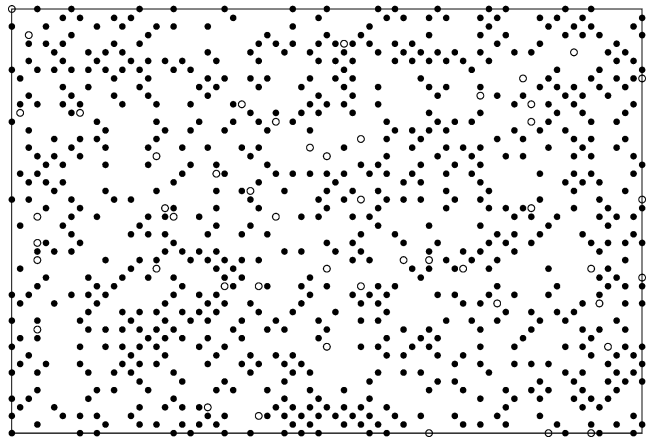

(a)

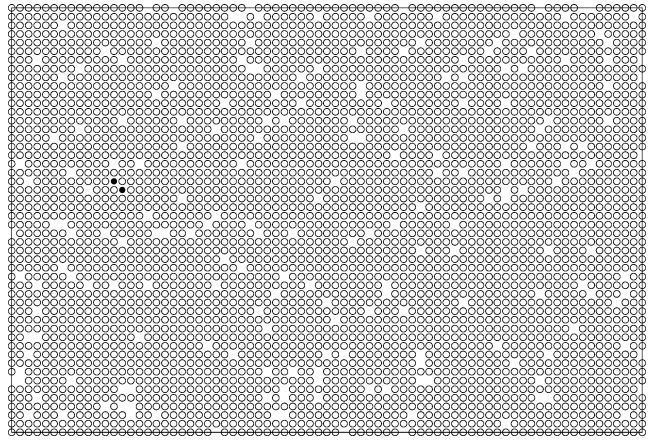

(b)

Fig. 2. Snapshots of the lattice for the MC run shown in Fig. 1a, at (a) $t = 1.5 \times 10^4$ and (b) $8.5 \times 10^4$ MCS. The open and filled circles indicate CO and O, respectively.

constant. This dependence is, however, very weak and insignificant for our conclusions.

Typical reaction kinetics and lattice snapshots obtained for the reference case in which there is no oxide formation (i.e., with $p_1^{ox} = 0$) are presented in Figs. 1 and 2. As expected, the surface is seen to be covered primarily by O at $O_2$ excess (Fig. 2a) and by CO at CO excess (Fig. 2b). If initially $O_2$ is in excess (Fig. 1a), the kinetic phase transition from the high reactive state (low CO coverage, high O coverage) occurs at 600 MCS just after increasing $p_{ad}^{CO}$ from 0.014 to 0.016. The reverse transition takes place at 700 MCS (Fig. 1b) after decreasing $p_{ad}^{CO}$ from 0.008 to 0.006.

To illustrate what may happen in the case of oxide formation, we show (Figs. 3 and 4) reaction kinetics and lattice snapshots calculated for $p_1^{ox} = 0.001$, $p_2^{ox} = 0.005$, $p_r = 0.1$, $p_{ox} = 0.01$, and $p_{red} = 0.01$. In this case, the surface is also almost exclusively covered by CO at CO excess (Fig. 4b). In the high-reactive state at $O_2$ excess, the surface is, however, covered primarily by $O^*$ (Fig. 4a) and the $CO_2$ formation occurs mainly via the apparent ER step (8). In fact, this means that in the latter case we have an oxide layer containing vacancies. The relative role of vacancies in oxide formation, i.e., the role of step (7) compared to step (5), depends on $p_{ad}^{CO}$. For example, step (7) slightly dominates for $p_{ad}^{CO} = 0.4$, because in this case the number of vacancies is appreciably higher than the number of adsorbed O atoms (Fig. 4a). With decreasing or increasing $p_{ad}^{CO}$, the role of vacancies increases or decreases, respectively.

The hysteresis loops corresponding to the kinetics exhibited in Figs. 1 and 3 are presented in Figs. 5a and 5b. Due

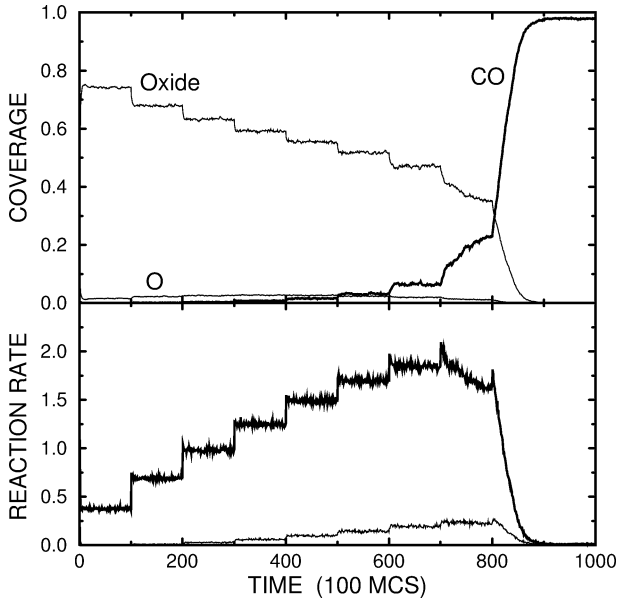


Fig. 3. Adsorbate coverages (ML) and reaction rate ($10^{-3}$ ML/MCS) for the reaction scheme with oxide formation for (a) increasing and (b) decreasing $p_{ad}^{CO}$ (between 0.005 and 0.5) by $\Delta p_{ad}^{CO} = 0.005$ after each $10^4$ MCS. The total reaction rate is shown by the thick line. The contribution of step (3) to the reaction rate is indicated by a thin line. (The method of calculation of the reaction rate is the same as in Fig. 1.)

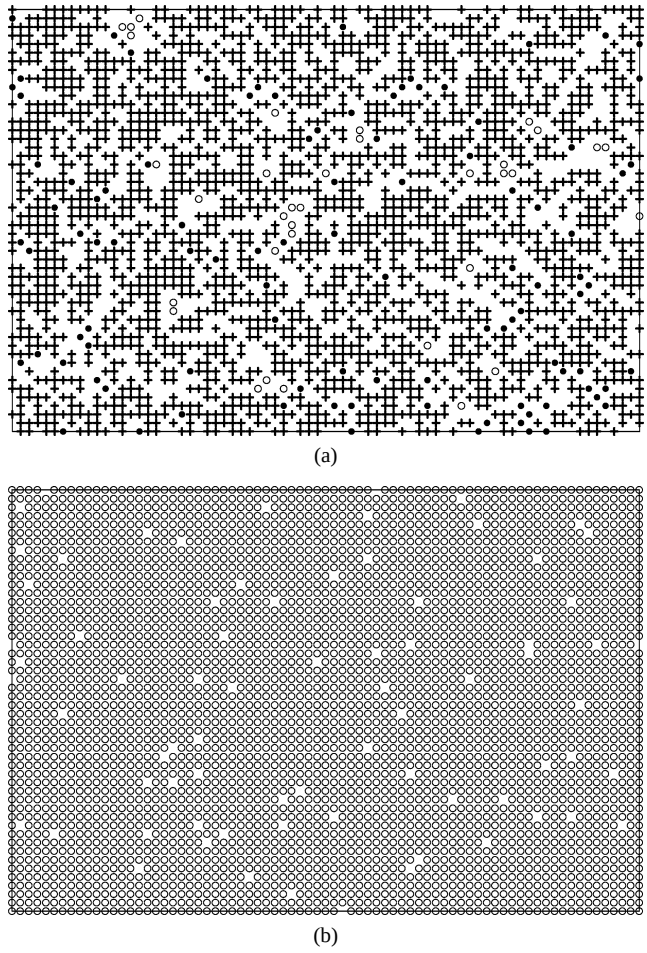


Fig. 4. Snapshots of the lattice for the MC run shown in Fig. 3a, at (a) $t = 3.5 \times 10^4$ and (b) $9.5 \times 10^4$ MCS. The open and filled circles and the plus signs indicate CO, O, and O*, respectively.

to the oxide formation, the loop is shifted by a factor of 3–4 to higher $p_{ad}^{CO}$ values (this suggests that the oxide formation helps in resisting CO-poisoning transition). The shapes of the loops are, however, similar. A major new feature is that in the oxide case the maximum reaction rate is 5 times lower compared to the case with no oxide. By decreasing the rates of oxide formation and removal, this difference may be further increased. If for example we keep the bulk of the parameters as in the case of Fig. 4 (or Fig. 5b) but decrease the probabilities of oxide formation and removal down to $p_1^{ox} = 0.0002$, $p_2^{ox} = 0.001$, and $p_r = 0.02$, the maximum reaction rate is about 30 times lower than that obtained with no oxide formation (cf. Figs. 5a and 5c; note also a slight shift of the hysteresis compared to that shown in Fig. 5b).

With increasing $p_r$ (e.g., up to $\simeq 1$), the maximum reaction rate will be about the same as in the case of Fig. 5a, but contrary to the experiment in [23] the oxide coverage will be low (due to rapid oxide removal).

## 4. Conclusion

In summary, we have presented MC simulations illustrating that the oxide formation and removal, running primarily with participation of gas-phase $O_2$ and CO molecules, may completely control the high reactive state of CO oxidation on Pt. In this case, the hysteresis loop is qualitatively similar to that predicted by the conventional reaction scheme (1)–(3), but it is shifted to higher $P_{CO}/P_{O_2}$ ratios and the maximum

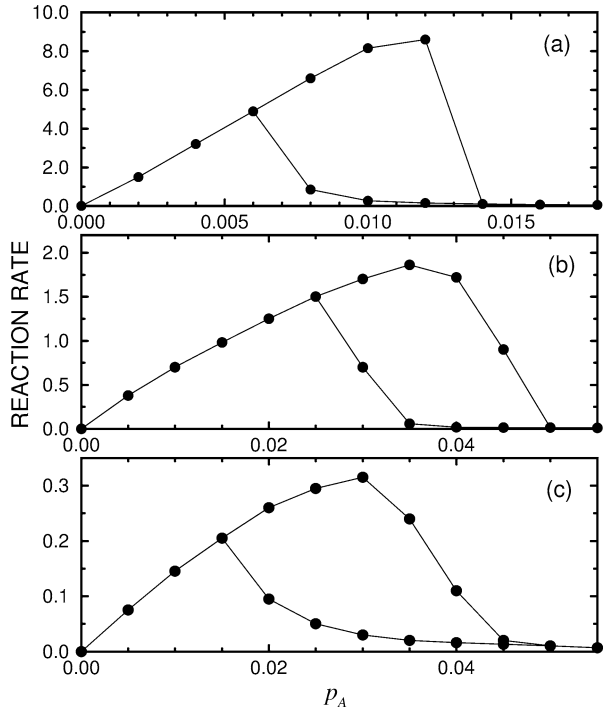


Fig. 5. Hysteresis loops in the reaction rate (a and b) for the kinetics shown in Figs. 1 and 3, respectively and (c) for the kinetics when the rates of oxide formation and removal are five times lower than in case (b). (Note that in order to label the horizontal axis we use $p_A$ instead of $p_{\mathrm{ad}}^{\mathrm{CO}}$.)

$CO_2$ formation rate in the high-reactive state is appreciably lower than the corresponding value in the absence of the oxide state. We believe that this is an interesting example illustrating that in the case of catalytic reactions with low- and high-reactive processes occurring in parallel the former may suppress the latter.

Whether during the high-reactive state the oxide formation and removal steps [(7) and (8)] are kinetically more stable compared to the conventional steps [(1)–(3)] depends on the ratio of the corresponding rate constants. Physically, it is clear that the oxide formation can be suppressed by reducing the rate constants of step (7). Alternatively, one can increase the rate constant of oxide removal (8). The latter may result in reduction of the oxide coverage and accordingly the conventional steps may become dominant.

In our analysis, we have used the MC technique, which makes it possible to take into account various cooperative effects inherent for oxide formation. In principle, one can, however, formulate a corresponding MF model. With a proper choice of the model-parameter values, it may also describe the key features of the reaction under consideration and accordingly be useful in applications.

Concerning applications, it is of interest to notice that the predicted oxide-induced shift of catalyst resistance to CO poisoning to higher CO pressures may be favorable for practical vehicle emission systems, provided that the accompanying decrease in the maximum $CO_2$-formation rate is not dramatic. For well-dispersed, supported Pt, the role of the oxidic oxygen may actually be more pronounced than for the bulk platinum, because supported Pt particles are more easily oxidized (note, however, that the situation depends also on the rate of oxide removal).

Finally, it is appropriate to articulate that our simulations were partly motivated by the STM studies [23] of CO oxidation on Pt(110) at atmospheric pressures. The main results of our simulations are in qualitative agreement with the experiment. Whether and under what conditions our model may be applicable to other faces remain open for debate. Applicability of the model to nanometer-sized supported catalyst particles is open for discussions as well, because such particles have primarily the (111) and (100) facets.

## Acknowledgments

The authors thank Per-Anders Carlsson for useful discussions. This work was supported by the Swedish Energy Agency (Grant P12554-1). The Competence Center for Catalysis is hosted by Chalmers University of Technology and financially supported by the Swedish Energy Agency and the member companies AB Volvo, Saab Automobile Powertrain AB, Johnson Matthey CSD, Perstorp AB, Akzo Catalyst, and MTC AB and the Swedish Space Corporation.

## References

[1] L.F. Razon, R.A. Schmitz, Catal. Rev. Sci. Eng. 28 (1986) 89.
[2] J.W. Evans, Langmuir 7 (1991) 2514.
[3] V.P. Zhdanov, B. Kasemo, Surf. Sci. Rep. 20 (1994) 111.
[4] M. Bär, Ch. Zülicke, M. Eiswirth, G. Ertl, J. Chem. Phys. 96 (1992) 8595.
[5] M. Berdau, G.G. Yelenin, A. Karpowicz, M. Ehsasi, K. Christmann, J.H. Block, J. Chem. Phys. 110 (1999) 11551.
[6] S. Wehner, F. Baumann, J. Küppers, Chem. Phys. Lett. 370 (2003) 126.
[7] G.K. Boreskov, Heterogeneous Catalysis, Nauka, Moscow, 1986.
[8] V.P. Zhdanov, B. Kasemo, Surf. Sci. Rep. 39 (2000) 25.
[9] V.P. Zhdanov, B. Kasemo, Catal. Lett. 72 (2001) 7.
[10] V.P. Zhdanov, B. Kasemo, Surf. Sci. 496 (2002) 251.
[11] D.J. Liu, J.W. Evans, J. Chem. Phys. 117 (2002) 7319.
[12] N. Pavlenko, R. Imbihl, J.W. Evans, D.J. Liu, Phys. Rev. E (2003) submitted for publication.
[13] V.P. Zhdanov, B. Kasemo, Appl. Surf. Sci. 74 (1994) 147.
[14] M. Rinnemo, D. Kulginov, S. Johansson, K.L. Wong, V.P. Zhdanov, B. Kasemo, Surf. Sci. 376 (1997) 297.
[15] S. Johansson, L. Österlund, B. Kasemo, J. Catal. 201 (2001) 275.
[16] P.-A. Carlson, Licentiate Thesis, Chalmers University of Technology, Göteborg, 2002.
[17] Under certain conditions, the kinetics of CO oxidation on Pt can also be complicated by carbon deposition [K.R. McCrea, J.S. Parker, G.A. Somorjai, J. Phys. Chem. B 106 (2002) 10854].
[18] B.C. Sales, J.E. Turner, M.B. Maple, Surf. Sci. 114 (1982) 381.
[19] A.L. Vishnevskii, V.I. Savchenko, Kinet. Catal. 31 (1990) 99.
[20] A. Von Oertzen, H.H. Rotermund, A.S. Mikhailov, G. Ertl, J. Phys. Chem. B 104 (2000) 3155.
[21] H.H. Rotermund, M. Pollmann, I.G. Kevrekidis, Chaos 12 (2002) 157.

[22] L. Olsson, E. Fridell, J. Catal. 210 (2002) 340.
[23] B.L.M. Hendriksen, J.W.M. Frenken, Phys. Rev. Lett. 89 (2002) 046101.
[24] J.H. Miners, S. Cerasari, V. Efstathiou, M. Kim, D.P. Woodruff, J. Chem. Phys. 117 (2002) 885.
[25] H. Over, Y.D. Kim, A.P. Seitsonen, S. Wendt, E. Lundgren, M. Schmid, P. Varga, A. Morgante, G. Ertl, Science 287 (2000) 1474.
[26] V.P. Zhdanov, Surf. Sci. Rep. 45 (2002) 231.
[27] V.P. Zhdanov, B. Kasemo, J. Catal. 214 (2003) 121.
[28] J.T. Stuckless, C.E. Wartnaby, N. Al-Sarraf, S.J.B. Dixon-Warren, M. Kovar, D.A. King, J. Chem. Phys. 106 (1997) 2012.
[29] M. Todorova, W.X. Li, M.V. Ganduglia-Pirovano, C. Stampfl, K. Reuter, M. Scheffler, Phys. Rev. Lett. 89 (2002) 096103.
[30] V.P. Zhdanov, B. Kasemo, Surf. Sci. 521 (2002) L662.